12

Computerization and Computer Algebra

12.1 Introduction

The quantized detector network (QDN) formalism was designed from the outset to deal with detector networks of arbitrary complexity and rank. However, there is a price to be paid. A qubit register of rank r is a Hilbert space of dimension 2^r, so the dimensionality of quantized detector networks grows exponentially with rank. For example, a relatively small system of, say, 10 detectors involves a Hilbert space of dimension $2^{10} = 1,024$.

Even such a relatively small system cannot be dealt with easily by manual calculation, because quantum mechanics (QM) involves entangled states. Labstates in QDN are far more complex (in the sense of having far more mathematical structure) than the corresponding states in a classical register of the same rank. Some of the mathematical entanglement and separability properties of quantum labstates are discussed in Chapters 22 and 23.

The quantum entanglement structure of labstates poses a ubiquitous and serious problem, for both theorists and experimentalists. At this time, there is significant interest in quantum entanglement, particularly regarding its use in quantum computing, but theoretical understanding of entanglement is still surprisingly limited.

On the experimental side, quantum computers with 2000 qubits are currently being developed (D-Wave Systems, 2016). There is scope here for the application of QDN to networks of rank going into the many thousands. For those sorts of systems under observation (SUOs), quantum entanglement makes calculations by hand far too laborious to be of any practical use.

Fortunately, three factors come to our aid here, making the application of QDN to large-rank networks a potentially viable proposition.

https://doi.org/10.1017/9781009401432.013 Published online by Cambridge University Press

Modularization

We saw in previous chapters that QDN deals with discrete aspects of observation, despite the fact that standard QM and relativistic quantum field theory (RQFT) deal with continuous degrees of freedom. This discreteness comes in three forms, referred to us as stages, nodes, and modules, and all of that is due to three inescapable physical facts. First, all real observations take time and involve discrete signals in finite numbers of detectors.[1] Second, real apparatus is constructed from atoms, not continua. Third, these atoms form finite numbers of well-characterized modules, as discussed in the previous chapter.

Contextuality

A critically helpful fact here is that in any particular experiment, the contextual subspaces that the observer needs to deal with will usually be of significantly lower dimensions than that of the full quantum registers involved. For example, while the register ground state $\mathbf{0}_n$ at stage Σ_n is an indispensable component of the QDN formalism, there are few situations that will involve the completely saturated labstate $\underline{\mathbf{2^r - 1}}_n \equiv \widehat{\mathbb{A}}_n^1 \widehat{\mathbb{A}}_n^2 \ldots \widehat{\mathbb{A}}_n^r \mathbf{0}_n$. This will certainly be the case when the rank r is large, say, of the order of hundreds or even possibly thousands.

Computerization

While QDN calculations can often be done by hand for small rank calculations involving a small number of stages, the use of computer algebra (CA) software, such as Maple, Mathlab, and Mathematica, allows problems with much greater rank registers running over many more stages to be dealt with. All but the simplest network calculations in this book were done using a computer algebra program developed by us called Program MAIN, for example.

12.2 Program MAIN

In this chapter we discuss the application of CA to QDN. We illustrate this approach to QDN by describing a typical experiment, referred to here as the *Wollaston interferometer* (WI), shown in Figure 12.1.

The aim in this experiment is to investigate the polarization structure of an unpolarized monochromatic beam of light. From source S, the beam is first passed through a Wollaston prism W that splits it into two orthogonally polarized components 1_1 and 2_1 as shown. Component 1_1 has "internal" polarization represented by ket $|s_1^1\rangle$ while component 2_1 has polarization state $|s_1^2\rangle$, orthogonal to $|s_1^1\rangle$. Component 1_1 is then deflected by mirror M to 1_2 and then toward one input channel of beam splitter B. Component 2_1, meanwhile, is passed through polarization rotator R^θ that rotates $|s_1^2\rangle$ into $\cos(\theta)|s_2^2\rangle + \sin(\theta)|s_2^1\rangle$, before passing

[1] Technically, the signals are not discrete or continuous. It is the observer who interprets whatever they find at a detector as a discrete bit of information.

https://doi.org/10.1017/9781009401432.013 Published online by Cambridge University Press

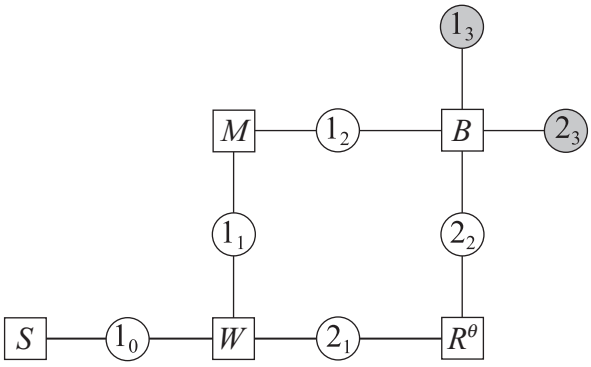

Figure 12.1. The Wollaston interferometer. A monochromatic, unpolarized beam of light from source S is passed through Wollaston prism W. Emerging polarized beam 1_1 is deflected by mirror M onto beam splitter B, while emerging polarized beam 2_1 has its polarization rotated by angle θ through module R^θ, before hitting B. Signal detection is at detectors 1_3 and 2_3.

into the other input channel of B. The two beam splitter outcome channels are monitored by final stage detectors 1_3 and 2_3. The angle θ is chosen by the observer before the preparation switch 1_0 is thrown.

If the transmission t and reflection r coefficients of the beam splitter B are known, then the observed outcome frequencies at the final stage detectors will depend on θ, and this gives information about the relative magnitudes of the two polarizations in the initial beam.

For applying QDN to the WI and all other experiments we have a single CA program, referred to here as *MAIN*. This program consists of two sections, A and B. In Section A, we input the details of the particular experiment we want to calculate, such as how many stages the experiment involves, the rank of each stage quantum register, and so on.

In practice, MAIN carries full details of all the experiments we have investigated, with a path parameter that allows us to select any experiment of current interest. For example, the path parameter for WI is 44.

Given the path parameter, MAIN jumps to Section A, initializing the variables from the relevant data there. Then MAIN jumps to Section B, automatically calculating everything of interest, such as the outcome probabilities at each final labstate detector.

The power of this approach is that all the work is done in encoding Section A. In general, this does not take long and is straightforward, given a stage diagram for the process and the module rules discussed in the previous chapters. Section B is universal, that is, is the same for all experiments. This gives a very economical and powerful approach indeed, allowing a great range of questions to be posed and answered rapidly. The only real theoretical problem is in deciding the stage-to-stage evolution operators $U_{n+1,n}$ in the encoding of Section A. This part of

https://doi.org/10.1017/9781009401432.013 Published online by Cambridge University Press

the process is currently where the computer does not help and the theorist has to decide what goes in. However, it should be possible to automate this part as well, if stage diagrams could be encoded first. We comment on this further, below.

12.3 The Wollaston Interferometer

We now describe the steps followed for a typical experiment, in this case the WI. This example illustrates the fact that MAIN can deal with *total* states, that is, entangled quantum states of the form

$$|\Psi_n) \equiv \sum_a |s_n^a\rangle \otimes \boldsymbol{i}_n^a, \tag{12.1}$$

where $|s_n^a\rangle$ is an "internal" SUO state, carrying information such as polarization, and $\boldsymbol{i}_n^a$ is a computational basis representation (CBR) labstate element carrying information about the signal state of the detectors.

Encoding

Our QDN notation is transcribed into program MAIN as follows. Although the observer's focus is the signality of the signal detector amplitudes, the internal calculations of MAIN are written in terms of the CBR. The reason is that labstates of signality greater than one are nonlinear in the signal operators $\widehat{\mathbb{A}}_n^i$, whereas the CBR is transparent to signality.

Our encoding takes the following form:

$$\begin{aligned} \boldsymbol{i}_n &\to a[i,n], \quad \overline{\boldsymbol{i}_n} \to A[i,n], \\ |s_n^p\rangle &\to s[p,n], \quad \langle s_n^p| \to S[p,n]. \end{aligned} \tag{12.2}$$

Here the symbols a, A, s, and S were arbitrarily chosen, with the rule that lowercase letters represent quantum "ket" states and capital letters represent their duals.

The power of the CA approach comes in at this point in that we can use differentiation to implement "inner product" rules. For example,

$$\overline{\boldsymbol{i}_n}\boldsymbol{j}_n \to \frac{\partial a[j,n]}{\partial a[i,n]} = \delta^{ij}, \quad \langle s_n^p | s_n^q\rangle \to \frac{\partial s[q,n]}{\partial s[p,n]} = \delta^{pq}, \tag{12.3}$$

which is readily encoded in CA.[2]

In the following, the asterisk symbol $*$ denotes ordinary commutative multiplication in the CA program. It is an important and helpful fact that our encoding does not need any noncommutative product operation, although CA is capable of handling those when required.

[2] Differentiation is a good example of the dichotomy between the continuous and the discrete. Mathematicians frequently deal with continuous variables, but mathematicians themselves operate on discrete principles: all of mathematics is done line by line, symbol by symbol, in a discrete way, very much like the way experimentalists have to operate in the real world.

https://doi.org/10.1017/9781009401432.013 Published online by Cambridge University Press

If r_n is the rank of the stage-Σ_n qubit register and d_n is the dimension of the internal SUO Hilbert space, also at that stage, then total states will be of the form

$$\begin{aligned} |\Psi_n) &\equiv \sum_{i=0}^{2^{r_n}-1} \sum_{p=1}^{d_n} c_n^{p,i} |s_n^p\rangle \otimes \boldsymbol{i}_n \\ \rightarrow \Psi[n] &\equiv \sum_{i=0}^{2^{r_n}-1} \sum_{p=1}^{d_n} c[p,i,n] * s[p,n] * a[i,n], \end{aligned} \tag{12.4}$$

while their duals are of the form

$$\begin{aligned} (\Phi_n| &\equiv \sum_{i=0}^{2^{r_n}-1} \sum_{p=1}^{d_n} D_n^{p,i} \langle s_n^p| \otimes \overline{\boldsymbol{i}_n} \\ \rightarrow \Phi[n] &\equiv \sum_{i=0}^{2^{r_n}-1} \sum_{p=1}^{d_n} D[p,i,n] * S[p,n] * A[i,n], \end{aligned} \tag{12.5}$$

where the $c_n^{p,i}$ and $D_n^{p,i}$ are complex coefficients (readily handled in CA).

Inner products are evaluated by the CA prescription

$$\begin{aligned} (\Phi_n|\Psi_n) \rightarrow & \sum_{i=0}^{2^{r_n}-1} \sum_{p=1}^{d_n} \frac{\partial^2 \Phi[n]}{\partial S[p,n] \partial A[i,n]} * \frac{\partial^2 \Psi[n]}{\partial s[p,n] \partial a[i,n]} \\ = & \sum_{i=0}^{2^{r_n}-1} \sum_{p=1}^{d_n} D[p,i,n] * c[p,i,n]. \end{aligned} \tag{12.6}$$

Draw a Stage Diagram

Having decided to model a particular experiment, we need to have a clear overview of the experiment's space-time architecture. That is best done graphically. Any quantum experiment can be described diagrammatically by a *stage diagram*, that is, a representation of the detectors and modules at each stage, with different stages linked by amplitude transmission lines.

Currently, MAIN has no facility for automatically transcribing such diagrams into code, but we envisage the development of graphical interface software that would make this part of the programming straightforward. The reason for this optimism is that there is only a finite variety of modules, and their properties can be well specified and catalogued mathematically, as discussed in Chapter 11. Figure 12.1 is the relevant diagram for the WI calculation.

Transcription Phase

Given the stage diagram, the next step is to read from it the following information and encode it into MAIN:

1. N, the number of stages, not counting the initial stage, which is labeled Σ_0. There is no limit to the size of N apart from the capacity limits of the

https://doi.org/10.1017/9781009401432.013 Published online by Cambridge University Press

computer. In our case, a personal computer with 32 gigabytes random access memory and a 240 gigabyte hard disc was quite sufficient to deal with all the experiments discussed in this book. For our WI calculation, $N = 3$.

2. $r[0], r[1], \ldots, r[N]$, the rank at each stage. From Figure 12.1 we have $r[0] = 1$, $r[1] = r[2] = r[3] = 2$.
3. $d[0], d[1], \ldots, d[N]$, the dimensions of the "internal" SUO Hilbert space at each stage. In the case of the WI, we have two orthonormal polarizations of light, $|s_n^1\rangle, |s_n^2\rangle$, to factor in. These are often taken as horizontal and vertical polarizations, but in principle could be circular polarizations if required. Hence we take $d[0] = d[1] = d[2] = 2$.
4. The initial labstate: for the WI being discussed, we take $|\Psi_0) \equiv \{c^1|s_0^1\rangle + c^2|s_0^2\rangle\} \otimes \mathbf{1}_0$, and its dual $(\Psi_0| \equiv \{c^{1*}\langle s_0^1| + c^{2*}\langle s_0^2|\} \otimes \overline{\mathbf{1}_0}$, where c^{i*} is the complex conjugate of c^i. The coefficients c^i characterize the two incident beam polarizations and satisfy $|c^1|^2 + |c^2|^2 = 1$.

   These states are encoded into MAIN as

$$\begin{aligned} |\Psi_0) &\to \psi[0] \equiv (c[1] * s[1,0] + c[2] * s[2,0]) * a[1,0], \\ (\Psi_0| &\to \Psi[0] \equiv (C[1]) * S[1,0] + C[2] * S[2,0]) * A[1,0]. \end{aligned} \tag{12.7}$$

   MAIN checks at each stage that normalization is preserved, so that at any stage Σ_n, we have

$$(\Psi_n|\Psi_n) = (\Psi_0|\Psi_0) \to C[1] * c[1] + C[2] * c[2]. \tag{12.8}$$

5. From Figure 12.1 and the rules of the modules concerned (covered in the previous chapter) we write (on paper)

   Stage $\Sigma_0 \to \Sigma_1$

$$\begin{aligned} U_{1,0}\left\{|s_0^1\rangle \otimes \widehat{\mathbb{A}}_0^1 \mathbf{0}_0\right\} &= |s_1^1\rangle \otimes \widehat{\mathbb{A}}_1^1 \mathbf{0}_1, \\ U_{1,0}\left\{|s_0^2\rangle \otimes \widehat{\mathbb{A}}_0^1 \mathbf{0}_0\right\} &= |s_1^2\rangle \otimes \widehat{\mathbb{A}}_1^2 \mathbf{0}_1. \end{aligned} \tag{12.9}$$

   Stage $\Sigma_1 \to \Sigma_2$

$$U_{2,1}\left\{|s_1^1\rangle \otimes \widehat{\mathbb{A}}_1^1 \mathbf{0}_1\right\} = |s_2^1\rangle \otimes \widehat{\mathbb{A}}_2^1 \mathbf{0}_2, \tag{12.10}$$

$$U_{2,1}\left\{|s_1^2\rangle \otimes \widehat{\mathbb{A}}_1^2 \mathbf{0}_1\right\} = (\cos\theta|s_2^2\rangle + \sin\theta|s_2^1\rangle) \otimes \widehat{\mathbb{A}}_2^2 \mathbf{0}_2. \tag{12.11}$$

   Stage $\Sigma_2 \to \Sigma_3$

$$\begin{aligned} U_{3,2}\left\{|s_2^1\rangle \otimes \widehat{\mathbb{A}}_2^1 \mathbf{0}_2\right\} &= |s_2^1\rangle \otimes \left(t\widehat{\mathbb{A}}_3^2 \mathbf{0}_3 + ir\widehat{\mathbb{A}}_3^1 \mathbf{0}_3\right), \\ U_{3,2}\left\{|s_2^1\rangle \otimes \widehat{\mathbb{A}}_2^2 \mathbf{0}_2\right\} &= |s_2^1\rangle \otimes \left(t\widehat{\mathbb{A}}_3^1 \mathbf{0}_3 + ir\widehat{\mathbb{A}}_3^2 \mathbf{0}_3\right), \\ U_{3,2}\left\{|s_2^2\rangle \otimes \widehat{\mathbb{A}}_2^2 \mathbf{0}_2\right\} &= |s_2^2\rangle \otimes \left(t\widehat{\mathbb{A}}_3^1 \mathbf{0}_3 + ir\widehat{\mathbb{A}}_3^2 \mathbf{0}_3\right). \end{aligned} \tag{12.12}$$

   Here t and r are beam splitter parameters, and we use (11.28).

https://doi.org/10.1017/9781009401432.013 Published online by Cambridge University Press

That is all the theoretical input needed. The next step is to transcribe it into Section A code.

6. To transcribe the above information, we first use contextual completeness to write down $U_{1,0}$, $U_{2,1}$, and so on, and then use the rules (12.2). For instance, from (12.9) this gives

$$\begin{aligned} U_{1,0} &= |s_1^1\rangle \otimes \widehat{\mathbb{A}}_1^1 \mathbf{0}_1 \langle s_0^1| \otimes \overline{\mathbf{0}_1} \mathbb{A}_0^1 + |s_1^2\rangle \otimes \widehat{\mathbb{A}}_1^2 \mathbf{0}_1 \langle s_0^2| \otimes \overline{\mathbf{0}_1} \mathbb{A}_0^1 \\ &= |s_1^1\rangle\langle s_0^1| \otimes \mathbf{1}_1 \overline{\mathbf{1}_0} + |s_1^2\rangle\langle s_0^2| \otimes \mathbf{2}_1 \otimes \overline{\mathbf{1}_0} \\ \rightarrow U[1,0] &\equiv s[1,1] * S[1,0] * a[1,1] * A[1,0] + \\ &\quad s[2,1] * S[2,0] * a[2,1] * A[1,0], \end{aligned} \tag{12.13}$$

and similarly for $U_{2,1}$ and $U_{3,2}$.

This is all the input we need to provide program MAIN for it to answer all possible maximal questions about this particular experiment.

Evaluation Phase

Once Section A has been initialized, Section B goes into action, employing several key procedures (subroutines):

1. Given $U[n+1,n]$ and $U[n+2,n+1]$, then the operator $U_{n+2,n} \equiv U_{n+1,n+1}\, U_{n+1,n}$ is given by the rule $U_{n+2,n} \rightarrow U[n+2,n]$, where

$$U[n+2,n] \equiv \sum_{i=0}^{2^{r[n+1]}-1} \sum_{p=1}^{d[n+1]} \frac{\partial^2 U[n+2,n+1]}{\partial S[p,n+1] \partial A[i,n+1]} * \frac{\partial^2 U[n+1,n]}{\partial s[p,n+1] \partial a[i,n+1]}. \tag{12.14}$$

   The overall contextual evolution operator $U[N,0]$ is evaluated by iterating this process.
2. The retraction operator $\overline{U}_{N,0}$ is calculated from $U[N,0]$ by complex conjugation of coefficients and the interchange $s \leftrightarrow S$, $a \leftrightarrow A$. Complex conjugation is readily handled in CA.
3. The detector POVM operators $E^i_{N,0} \rightarrow E[i,N]$ discussed in Chapter 9 are calculated by the rule

$$E[i,N] \equiv \sum_{p=1}^{d[N]} \frac{\partial^2 \overline{U}[N,0]}{\partial S[p,N] \partial A[i,N]} * \frac{\partial^2 U[N,0]}{\partial s[p,N] \partial a[i,N]}. \tag{12.15}$$

   These should satisfy the rule

$$\sum_{i=0}^{2^{r[N]}-1} E[i,N] = \sum_{p=1}^{d[0]} s[p,N] * S[p,N] \sum_{i=0}^{2^{r[0]}-1} a[i,0] * A[i,0], \tag{12.16}$$

   which is a representation of I_0, the contextual identity operator at stage Σ_0. In MAIN, this is used as a useful check on the evolution operators $U[n+1,n]$ written down in Section A.

https://doi.org/10.1017/9781009401432.013 Published online by Cambridge University Press

4. The outcome probabilities $P(\boldsymbol{i}_N|\Psi_0)$, $i = 0, 1, 2, \ldots, 2^{r[N]} - 1$ are given by the rule (9.59) and are readily evaluated in MAIN, again using differentiation in the taking of inner products and operator action on state vectors. This gives the answers to all the 2^{r_N} maximal questions. Because large-rank stages may have excessive dimensions, the program gives a listing only of the nonzero answers to the maximal questions. This listing will generally be significantly smaller than the full potential set of answers, reflecting the fact that experiments generally deal with contextual subspaces of quantum registers, not the complete registers.

Points to note are the following.

Answers

Answers can be either in numerical form or in the far more useful algebraic form. For example, the output listing for the Wollaston interferometer is

$$P(\widehat{\mathbb{A}}_3^1\mathbf{0}_3|\Psi_0) = |c^1|^2r^2 + |c^2|^2t^2 + i(c^{2*}c^1 - c^{1*}c^2)rt\sin\theta,$$
$$P(\widehat{\mathbb{A}}_3^2\mathbf{0}_3|\Psi_0) = |c^1|^2t^2 + |c^2|^2r^2 - i(c^{2*}c^1 - c^{1*}c^2)rt\sin\theta. \qquad (12.17)$$

These sum to unity, as expected. The implication here is that MAIN has found the other two potential probabilities $P(\mathbf{0}_3|\Psi_0)$ and $P(\widehat{\mathbb{A}}_3^1\widehat{\mathbb{A}}_3^2\mathbf{0}_3|\Psi_0)$ to be zero.

Signal Decomposition

The CBR is excellent for CA but not so helpful with understanding signality. To assist in the interpretation, MAIN converts CBR probabilities into a listing of total signal probability for individual final-stage detectors, excluding any that have probabilities of zero. This gives valuable insight into the patterns of information flow. With some experience, it becomes clear why the photon concept has become so popular: signality is conserved in many quantum optics experiments unless some specific module such as a nonlinear crystal that creates photons is used, as in parametric down-conversion.

Partial Questions

MAIN answers the full set of maximal questions. We have stated before that this set of answers allows all partial questions to be answered. Therefore, CA gives us the possibility of answering all possible questions in the context of QDN. This becomes important in several complex experiments, such as the two-photon interferometer of Horne, Shimony, and Zeilinger (Horne et al., 1989) and the double-slit quantum eraser of Walborn et al. (Walborn et al., 2002), experiments covered in detail in Chapter 14.

12.4 Going to the Large Scale

There is little doubt in our mind that the greatest challenge facing quantum physics lies not with the reductionist laws of physics, which have been determined

https://doi.org/10.1017/9781009401432.013 Published online by Cambridge University Press

empirically to be excellent, but with the relatively unexplored laws of complexity and emergence. Even the simplest of experiments, such as the double-slit (DS) experiment discussed in Chapter 10, poses a serious challenge to QDN, simply because the dimensions of quantum registers grow exponentially with rank. With reference to Figure 10.2, suppose we wanted to model a DS experiment with K detector sites on screen. Three possible approaches that we could take are the following.

Approach 1: The *Theoretical* Approach
Here K is regarded as fixed but undetermined, and treated algebraically by the theorist on paper.

Approach 2: The *Brute Force* CA Approach
Here K is given a specific value, such as $K = 20$ in a CA program such as MAIN, and a relatively laborious calculation is done by a computer.

Approach 3: The *Symbolic* Approach
Here K is encoded symbolically and treated as an algebraic parameter characterizing the experiment. CA does in principle have the potential to handle this approach, but it requires more sophisticated programming, because that would essentially be an attempt to simulate the way the human theorist handles abstract modeling. A good example is that theorists can with training readily discuss infinite-dimensional Hilbert spaces on paper, but CA cannot easily handle infinities directly.

Approach 1 works for the relatively simple DS experiment but is impractical for other large-rank networks, prompting the development of the CA approach.

Approach 2 has definite limitations. A CA simulation of the DS experiment using MAIN was done with a range of values of K and timed. The results are given in the following table:

Rank r	T_r (seconds)
10	0.137
12	0.515
14	2.609
16	11.73
18	40.92
20	192.3
22	1284

Analysis of this table suggests that the time T_r for MAIN to complete a DS simulation with a rank-r screen register is approximately of the form $T_r = A + B2^r$, where A and B are constants. It is clear that even a rank-100 simulation could not be completed on this basis.

https://doi.org/10.1017/9781009401432.013 Published online by Cambridge University Press

Approach 3 should be made to work if contextual subspaces are incorporated adequately (which they are not, currently, in our program MAIN).

Three conclusions can be drawn from this analysis:

1. Computerization seems inevitable.
2. Computerization will be very useful in a broad range of problems, but some problems may remain intractable.
3. Intelligent use of contextual subspaces will be necessary for problems where the rank is too large for the brute force approach to work.

12.5 Prospects

Our current CA program, MAIN, requires the user to transcribe "by hand" the information contained in a stage diagram into CA form. This process could be, and perhaps should be, fully automated, opening the door to potentially vast applications. Ideally, this would utilize the currently accessible technology of touch screens, whereby the user used electronic graphics pens to sketch stage diagrams in freehand. These would then be automatically transcribed into the information currently fed in by hand in Section *A* of MAIN.

We envisage the development of user-friendly graphical software that would allow the user to select all the necessary modules that were of interest, using palettes of symbols representing real and virtual detectors, modules of all sorts, and lines representing transmission through various media. With the right information, it should be possible to encode different material properties, so that quantized detector networks representing crystals, glasses, and other complex systems such as neural networks and retinas could be dealt with in a systematic and coherent way.

There is little doubt in our mind that such an approach to complex problems involving quantum mechanical effects in engineering, materials science, and medical science will one day become commonplace.